# Site selectivity in $ZrO_2$-doped $Y_2O_3$ evidenced by x-ray absorption spectra calculations



1994 J. Phys.: Condens. Matter 6 8341

(http://iopscience.iop.org/0953-8984/6/40/025)

J. Phys.: Condens. Matter 6 (1994) 8341–8348. Printed in the UK

# Site selectivity in $ZrO_2$-doped $Y_2O_3$ evidenced by x-ray absorption spectra calculations

J P Crocombette and F Jollet

CEA, DSM, DRECAM, SRSIM, Centre d'Etudes de Saclay, 91191 Gif-sur-Yvette Cedex, France

Received 4 May 1994, in final form 21 June 1994

**Abstract.** The doping of $Y_2O_3$ by $ZrO_2$ leads to two possible sites for Zr cation substitution. Configuration-interaction-based calculations of the cation $L_2$ x-ray absorption edge shape of $Y_2O_3$, $ZrO_2$ and $ZrO_2$-doped $Y_2O_3$, explicitly taking into account the exact first-neighbour surrounding of the cation acting through crystal-field splitting and hopping terms, allows us to predict a site selectivity for Zr in the substitution for Y atoms.

## 1. Introduction

Yttrium oxide is a highly refractory material the use of which is increasing in several technological areas such as electronics and optics. Point defects in $Y_2O_3$, such as oxygen vacancies or cation impurities, have been studied both from a thermodynamic point of view [1] and by experimental and theoretical approaches of the electronic structure [2–4].

In previous work [5], we have shown on the basis of an extended x-ray absorption fine structure (EXAFS) study that, when $Y_2O_3$ is doped with $ZrO_2$, the Zr cations are substituted for the Y cations. As there are two yttrium sites in $Y_2O_3$ (see section 3), there are two possible substitution sites for Zr cations. In this paper, we focus on the question of the equivalence of these sites or of a possible site selectivity that could not be evidenced by EXAFS results. For this, we concentrate on the cation $L_2$ x-ray absorption spectroscopy (XAS) edge shape in $Y_2O_3$, monoclinic $ZrO_2$ and $ZrO_2$-doped $Y_2O_3$, for which the experimental results have already been published [5]. In fact, it is known that the shape of the 2p XAS edges depends strongly on the surrounding of the absorbing atom [6]. We present here configuration interaction calculations of the $L_2$ XAS edge shape; indeed, even if the electronic structure of transition-metal compounds can be in certain cases partially described by single-particle models, in the widely accepted model for the interpretation of the properties of transition-metal compounds, the so-called ZSA model [7], the emphasis is laid on the relative importance of intra-cationic d–d electronic repulsion versus band-structure quantities. So, in order to reproduce excitation spectra, it proves necessary to use multi-electronic approaches [8] which describe the material in terms of d-electron configurations and enable one to take into account the electronic interactions because, for instance, of Slater integrals or Racah parameters [9]. In the literature, calculations are made on clusters for which the surroundings of the cation are assumed to have perfect $O_h$ symmetry, i.e. to be either perfectly octahedral or cubic. The ionic limit, assuming no charge transfer, was used in the multiplet model of 2p XAS [10], while configuration interaction methods are used for metal 2p or 3p x-ray photoemission spectroscopy (XPS) or XAS [11], bremsstrahlung isochromat spectroscopy (BIS) [12] and valence band XPS [13]. However, in many cases,

0953-8984/94/408341+08$19.50  

the approximation of a perfect $O_h$ symmetry is not relevant, for instance when the cation site is distorted with respect to this symmetry. Starting from the approach in [13], we have developed a model to reproduce excitation spectra (metal 2p XAS and XPS, d-electron addition or removal of spectral weights), the interest of which is that it deals with any real surroundings, which enables us to consider low-symmetry cases, as encountered in particular oxides such as monoclinic $ZrO_2$, and that the covalency of the oxide is taken into account through the hopping terms. We present the description of the calculation method in section 2 while section 3 is devoted to the calculated $L_2$ x-ray absorption spectra of $Y_2O_3$, $ZrO_2$ and $ZrO_2$-doped $Y_2O_3$, and to discussion.

## 2. Calculation method

We consider a cluster made up of a central transition-metal cation surrounded by its oxygen first neighbours. The ions are in exact positions relative to each other. The 2p orbitals of the oxygen atoms and the d orbitals of the cation are considered to form the configuration basis. In the ionic picture the cation is assumed to bear its formal valence charge, leading formally to $d^n$ configurations. The presence, in the solid, of surrounding atoms induces two main phenomena. Firstly, the crystal field, i.e. electrostatic influence of first neighbours, lifts the degeneracy of cation d orbitals. Secondly, charge transfer produces a configuration interaction, leading to a mixing of $d^n$, $d^{n+1}\underline{L}$, $d^{n+2}\underline{L}^2$, ... where $\underline{L}$ denotes a hole in the ligand band. In the case of the $L_2$ edge of the cation, even for $d^0$ compounds, this may lead to the presence of two d electrons on the cation and therefore to d-electron interactions. Configurations with more than two ligand holes have been neglected in our calculations. The multi-electronic ground-state wavefunction of the cluster is therefore written

$$|\phi_g\rangle = \sum_i a_i|(d^n)_i\rangle + \sum_j b_j|(d^{n+1}\underline{L})_j\rangle + \sum_k c_k|(d^{n+2}\underline{L}^2)_k\rangle$$

where $i$, $j$, $k$ run over the Slater determinants forming the $d^n$, $d^{n+1}\underline{L}$ and $d^{n+2}\underline{L}^2$ configurations, respectively.

The Hamiltonian of the system takes into account the charge transfer through hopping terms, the crystal-field splitting and the intra-cationic electronic repulsions.

### 2.1. *The crystal field*

Since the surroundings are exact oxygen first neighbours, it proves possible to calculate the lifting of degeneracy of the cation d orbitals due to the surrounding charges (the so-called crystal-field splitting). As this splitting plays an important role in our results, we recall details of its calculation.

We consider only the d orbitals on the cation. Each oxygen ion is assimilated to a point bearing a formal charge of $-2e$ corresponding to an ionic picture of the solid. Following Figgis [14], an electron at point $r$ on a cation d orbital will sustain from one of these charges, situated at point $a$, a potential energy $V$ the matrix elements of which can be written in the spherical harmonics d basis set:

$$\langle m_1|V|m_2\rangle = \sum_{l=0}^{\infty}\sum_{m=-l}^{l}\frac{2e^2}{\epsilon_0(2l+1)}\frac{Y_l^{m*}(\theta_a,\phi_a)}{a^{l+1}}\left(\int R_{n,2}^2 r^{l+2}\,\mathrm{d}r\right)$$
$$\times\left(\iint Y_l^{m_1^*}(\theta,\phi)Y_l^{m}(\theta,\phi)Y_l^{m_2}(\theta,\phi)\sin\theta\,\mathrm{d}\theta\,\mathrm{d}\phi\right).$$

We note that $|m\rangle = R_{n2}Y_2^m$, $m$ ranging from 1 to 5, $R_{n2}$ being the unknown radial distribution of the d orbitals and $Y_2^m$ being a d spherical harmonic. The angular integral can be expressed with the $3j$ symbol. It is non-vanishing for $l = 0$, 2 or 4. The radial integral is formally equal to the mean value of $r^l$ and is denoted $\overline{r^l}$.

The term corresponding to $l = 0$ is equal to $(2e^2/4\pi\epsilon_0 a)\delta_{m_1,m_2}$.

The summation of this term over all neighbours of the cation in the real crystal would result in the so-called Madelung field. It is well known that this Madelung field depends strongly on the long-range surroundings of the cation, which can be easily seen from the fact that it varies with the interatomic distance as $a^{-1}$. Approximating the whole Madelung field by the first-neighbours part of it would be far too crude, but this term is diagonal and constant over d orbitals and so produces no splitting of these orbitals. As we are interested only in the splitting of these d orbitals, we do not take this term ($l = 0$) into account.

On the contrary the remaining terms ($l = 2, l = 4$), which lift the degeneracy of the d orbitals, vary with the interatomic distance as $a^{-3}$ and $a^{-5}$, respectively. So it is valid for these two terms to consider only the first-neighbour surroundings.

The total crystal field is then the sum over all oxygen neighbours of the $l = 2$ and $l = 4$ parts of the potential created by each of them. The two quantities $\overline{r^2}$ and $\overline{r^4}$ remain undefined. As explained by Figgis (p 38 of [14]), they cannot be properly connected to the actual values of the means of $r^2$ and $r^4$. So they have been treated as parameters in our calculation. The resulting $5 \times 5$ matrix is diagonalized, leading to eigenvalues and eigenvectors of the crystal field. Should the case arise for degenerate eigenvalues, one set of eigenvectors is arbitrarily chosen. What is obtained at the end is a set of five vectors, labelled from $\delta = 1$ to $\delta = 5$, with crystal-field energy $\Delta_\delta$. These vectors constitute, from now on, the d-orbital basis set.

### 2.2. *Total Hamiltonian*

The exact positions of oxygen atoms also enable one to calculate the oxygen–cation and oxygen–oxygen hopping terms for each pair of atoms of the cluster. Oxygen 2p orbitals are expressed in the usual $p_x$, $p_y$, $p_z$ basis set. The hopping matrix elements $V_{p\delta}$ and $V_{pp'}$ are calculated according to Slater and Koster [15] which take into account the relative geometries of the orbitals. The radial dependence of these terms are calculated from Harrison's [16] formulae used in the tight-binding method.

Concerning electronic interactions, the two-electron integrals $U_{\delta_4\delta_3\delta_2\delta_1}$ are expressed using Slater integrals or Racah parameters that are tabulated [3].

The total Hamiltonian of the cluster is then written out in the basis of Slater determinants:

$$H = \sum_{\delta\sigma}(\epsilon_d+\Delta_\delta)C^+_{\delta\sigma}C_{\delta\sigma}+\sum_{p,\sigma}\epsilon_p C^+_{p\sigma}C_{p\sigma}+\sum_{p,\delta,\sigma}(V_{p\sigma}C^+_{\delta\sigma}C_{p\sigma}+V^*_{p\delta}C^+_{p\sigma}C_{\delta\sigma})+\sum_{p,p',\sigma}V_{pp'}C^+_{p'\sigma}C_{p\sigma}$$
$$+\sum_{\substack{\delta_1,\delta_2,\delta_3,\delta_4\\ \sigma,\sigma'}}U_{\delta_4\delta_3\delta_2\delta_1}C^+_{\delta_4\sigma}C^+_{\delta_3\sigma'}C_{\delta_2\sigma'}C_{\delta_1\sigma}$$

where $\delta$ runs over the d orbitals, p runs over the oxygen 2p orbitals and $\sigma$ runs over the spins up or down. $C^+_{\alpha\sigma}$ and $C_{\alpha\sigma}$ are the electron creation and annihilation operators in the $\alpha\sigma$ state. The $\epsilon_d$ and $\epsilon_p$ are the atomic energies of cation d and oxygen 2p orbitals as listed in Harrison's [16] solid state table.

### *2.3. Spectrum calculation*

The results given hereafter concern the metal 2p XAS of $Y_2O_3$, $ZrO_2$ and $ZrO_2$-doped $Y_2O_3$, which have a formal valency of $4d^0$; the 2p x-ray absorption spectrum is dominated by dipole-allowed transitions to d and s final states. Owing to the larger wavefunction overlap the d channel is much stronger than the s channel [17]. Subsequently this latter is neglected. As far as the electronic structure is concerned, 2p XAS can be viewed as the annihilation of a metal 2p electron and the creation of a d electron. The annihilation part of the process is not included in our calculations. Core hole lifetime broadenings, as tabulated in [18], have been taken into account in our calculations. The x-ray absorption spectrum is then expressed as a summation over all final states $f$:

$$F(E) = \sum_f \sum_{\delta,\sigma} |(f|C^+_{\delta,\sigma}|g)|^2 L(E - E_F + E_g)$$

$L$ being the Lorentzian broadening and $g$ the calculated ground state.

The spectrum is not divided into $L_2$ and $L_3$ edges, this separation being due to cation 2p spin–orbit coupling. We also neglect the interactions between the core hole and the d electrons. Indeed for 4d transition metals the screening of the 2p core hole is quite effective. Moreover for $d^0$ compounds, atomic calculations by de Groot *et al* [19] show that the electron–hole interactions split the $L_3$ edge, but not the $L_2$ edge. This latter is split only when a crystal field is applied. So the theoretical spectra that we obtain will be compared with experimental $L_2$ edges. Of all the numerical quantities that are involved in the Hamiltonian, only $\overline{r^2}$ and $\overline{r^4}$ have been treated as variable parameters to fit the experimental spectra. The others (Racah parameters, $\epsilon_d$ and $\epsilon_p$) were deduced from tables for each material and kept constant.

## 3. Calculated spectra

### *3.1. Monoclinic zirconia*

The monoclinic zirconium dioxide structure is derived from the tetragonal structure by rotating the $c$ axis in the vertical plane so as to form with the $a$ axis an angle $\beta$ equal to 99°15′. The cell parameters are $a = 5.169$ Å, $b = 5.232$ Å and $c = 5.341$ Å. The unit cell contains 12 atoms (four Zr and eight O) [20]. The experimental $L_2$ edge [5] is well reproduced by our calculations. In particular the occurrence of a peak lying between the two main peaks is demonstrated (figure 1). The set of parameters used to fit the experimental spectrum is reported in table 1. The structure of this spectra can be explained by the uncommon first coordination of Zr atoms. The local structure around Zr can be represented as follows: the Zr atom is located at the centre of a cube and has seven oxygen neighbours, three oxygen atoms (labelled $O_I$) on the upper face of the cube and four oxygen atoms (labelled $O_{II}$) on the vertices of the lower faces of the cube, as depicted in the inset of figure 1. On the upper face, one oxygen atom is located at a vertex, while the two others are at the centre of the two remaining edges. In the real crystal, the $O_I$ oxygen atoms are slightly shifted from ideal positions. The Zr–$O_I$ distances range from 2.04 to 2.26 Å, the mean Zr–$O_{II}$ distance being 2.17 Å. These uncommon surroundings produce on d orbitals an uncommon crystal-field splitting; two nearly degenerate orbitals lie at lower energies, one orbital is unaffected and two nearly degenerate orbitals lie at higher energies. This

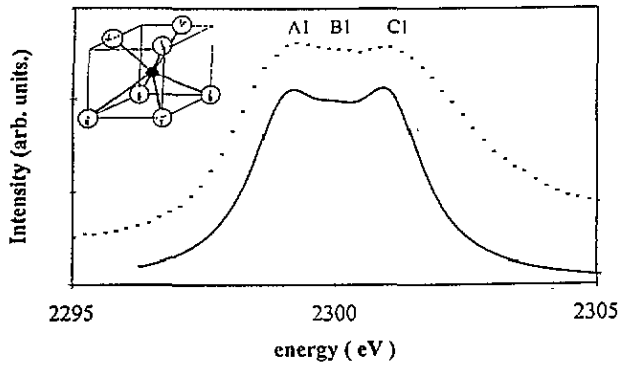


**Figure 1.** Zr $L_2$ edge in monoclinic $ZrO_2$: ——, theoretical; – – –, experimental. The inset shows the Zr coordination polyhedron in monoclinic $ZrO_2$ (idealized).

**Table 1.** Parameters used to fit the different $L_2$ experimental edges.

| | $\overline{r^2}$ ($Å^2$) | $\overline{r^4}$ ($Å^4$) |
|---|---|---|
| $ZrO_2$ | 0.6 | 1.7 |
| $Y_2O_3$ | 1.0 | 2.75 |

division of the d orbitals into three sets creates, for the spectrum, an equivalent splitting into three peaks.

Calculations with no charge transfer or no crystal field have been performed to highlight their relative effects on the spectral shape. If the crystal field is turned off, a very small splitting of the spectrum into five peaks is obtained, but the middle peak bears one half of the total spectral weight, and the spectrum cannot be compared with the experimental spectrum. If charge transfer is turned off, i.e. if the oxide is assumed to be in the ionic configuration, the theoretical spectrum follows directly from the diagonalization of the crystal field. In that case it does present the three peaks of the experimental edge but the energy separation between the peaks is reduced by a factor of roughly 40% from the complete calculation peak. A change in the parameters $\overline{r^2}$ and $\overline{r^4}$ restores the splitting between the two main peaks, but the position of the middle peak and the weight repartition are distorted. The structure of the spectrum can therefore be directly related to the exact crystal-field splitting. However, we proved that the charge-transfer effect should not be neglected. So, it proves necessary to consider both the exact crystal-field splitting and the charge transfer to account for the metal $L_2$ edge of this compound.

### *3.2. Yttrium oxide*

In view of tackling the substitution of Zr for Y in $Y_2O_3$ we have to consider, in a preliminary study, the case of the 2p XAS of yttrium in yttrium oxide. $Y_2O_3$ crystallizes into the C-type rare-earth sesquioxide structure closely related to the fluorite structure with a cell parameter $a = 10.604$ Å. The unit cell contains 80 atoms. In the fluorite lattice, each cation is surrounded by eight anions located at the vertices of a cube. The C-type structure is derived from it by removing one quarter of the anions and slightly rearranging the remaining anions. Two different cation first-neighbour surroundings exist. For 75% of the cations (called type I in the following), the vacancies lie at the end of a face diagonal, while for the other 25%

(called type II), they lie at the end of a body diagonal (see insets in figure 2). The real positions of the atoms are slightly shifted from the cube vertices. For the $Y_I$ atoms the distances to their first oxygen neighbours range from 2.24 to 2.33 Å. For the $Y_{II}$ atoms the distance is equal to 2.28 Å. We therefore had to consider two different clusters, leading to two different spectra. Type I and type II spectra look quite similar (see figure 2(a)). They are both constituted of two peaks, the second being smaller than the first. Type II is different from type I in that the splitting between the peaks is larger and in that the second peak is less intense. It should be stressed that, in both cases, these peaks do not correspond to a separation of the d orbitals into $t_{2g}$ and $e_g$ orbital sets, but to particular separations due to the particular atomic arrangements of the oxygen atoms. To obtain the theoretical spectrum a summation of the two spectra was made, with a ratio of 3 for type I to 1 for type II. This total spectrum was fitted to the experimental $L_2$ edge from [5] (see figure 2, curve (b) and (c), and table 1).

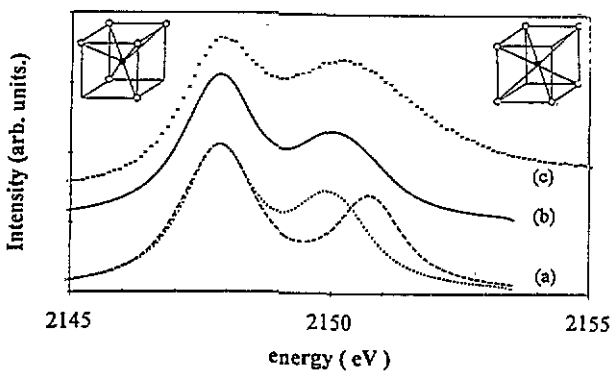


**Figure 2.** (a) $L_2$ edge for type I cluster (·····) and type II clusters (– – –) in $Y_2O_3$. (b) Theoretical Y $L_2$ edge for $Y_2O_3$, i.e. summation of type I and type II spectra with a ratio of 3 for type I to 1 for type II. (c) Experimental Y $L_2$ edge for $Y_2O_3$. The insets show on the left-hand side a type I cluster and on the right-hand side a type II cluster (idealized).

### *3.3. $ZrO_2$-doped $Y_2O_3$*

As the $L_2$ edges of $ZrO_2$ and $Y_2O_3$ are satisfactorily reproduced, we tackle the case of $ZrO_2$-doped $Y_2O_3$. This system has already been discussed in [5]. On the basis of an EXAFS study, it was found that Zr ions are substituted for Y ions. The local symmetry around Zr, which happens to be sixfold coordinated (it is sevenfold coordinated in $ZrO_2$), is the same as around Y in $Y_2O_3$. However, the Zr–O distances (2.17 Å) are smaller than the Y–O distances (2.27 Å) and are very close to those of the Zr–O distances in monoclinic $ZrO_2$. As EXAFS provides information only about the radial distribution of neighbours around the absorbing atom, that study did not evidence any site selectivity of the doping.

*In order to do so, we built two clusters, centred on Zr ions, from the two possible* clusters for $Y_2O_3$, assuming that, when Zr is substituted for Y, the only modification of the first-neighbour surroundings is an isotropic reduction in the distances by a factor of 2.17/2.27. We also assumed that all the parameters that were obtained for Zr in $ZrO_2$ (the crystal-field parameters $\overline{r^2}$ and $\overline{r^4}$ and the Racah parameters) are the same for Zr in $Y_2O_3$, these parameters being ionic properties of Zr ions, so that no parameter fit has been made.

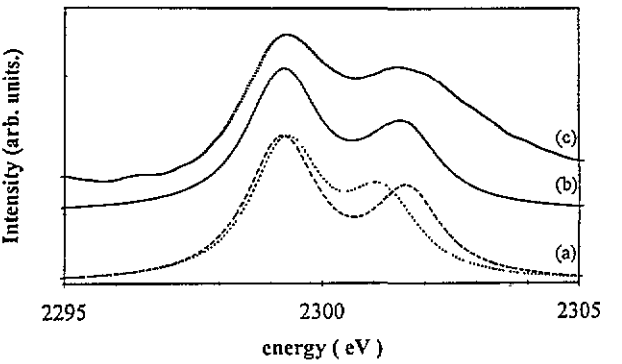


**Figure 3.** (a) $L_2$ edge for type I cluster (·····) and type II clusters (– – –) in $ZrO_2$-doped $Y_2O_3$. (b) Summation of type I and type II spectra with a ratio of 1 for type I to 3 for type II. (c) Experimental Zr $L_2$ edge in $ZrO_2$-doped $Y_2O_3$.

In figure 3, curves (a) and (c), are reported the theoretical spectra for both clusters and the experimental Zr $L_2$ spectrum from Thromat *et al* [5], respectively. The shapes of these spectra (both theoretical and experimental) do not resemble those for Zr in monoclinic $ZrO_2$. On the contrary they look very close to those of pure $Y_2O_3$, indicating that the shape of the $L_2$ edge results from the local arrangement around the cation.

**Table 2.** Energy separation between the peaks of $L_2$ edges in $ZrO_2$-doped $Y_2O_3$.

| Energy separation (eV) | | |
|---|---|---|
| Experimental | Type I cluster | Type II cluster |
| 2.2 | 1.84 | 2.38 |

The energy separations between the peaks are denoted by $\Delta_{exp}$ for the experimental spectrum and by $\Delta_I$ and $\Delta_{II}$ for type I and type II clusters, respectively. $\Delta_{II}$ is found to be closer to $\Delta_{exp}$ than is $\Delta_I$ (see table 2). If we assume an indifferent substitution of Zr for Y ions, the global theoretical spectrum is obtained, as in $Y_2O_3$, by a summation of type I and type II spectra with a ratio of 3 to 1. This leads to a separation, close to $\Delta_I$, which does not fit $\Delta_{exp}$ correctly. Different ratios have been tested, leading to different splittings. To obtain a theoretical splitting equal to the experimental splitting, it is necessary to make a summation with an approximate ratio of 3 for type II to 1 for type I (see figure 3, curve (b)). We interpret this as evidence of site selectivity for Zr in $Y_2O_3$; the Zr ions are more probably substituted for type II Y ions than for type I Y ions. Further neutron diffraction experiments will allow us to check this point in the near future.

In conclusion, taking into account the exact local order of the metal ion in a configuration interaction calculation, we reproduced the $L_2$ x-ray absorption edge of Zr in $ZrO_2$ and Y in $Y_2O_3$. We have stressed that exact crystal-field splitting is responsible for the overall shape of these $L_2$ edges but also that charge-transfer effects should not be neglected to account for them. Dealing with the case of $ZrO_2$-doped $Y_2O_3$, we found evidence of a possible site selectivity for Zr in its substitution for Y atoms.

## Acknowledgments

We would like to thank Professor G A Sawatzky and Dr H Eskes for providing a configuration interaction code dealing with a transition metal ion in an $O_h$ symmetry site. We are grateful to Dr F M F de Groot for fruitful discussions.

## References

[1] Norby T 1987 *Adv. Ceram.* **23** 107
[2] Jollet F, Noguera C, Thromat N, Gautier M and Duraud J P 1990 *Phys. Rev.* B **42** 7587
[3] Jollet F, Noguera C, Gautier M, Thromat N and Duraud J P 1991 *J. Am. Ceram. Soc.* 74 358–64
[4] Ching W Y and Yong-Nian Xu 1990 *Phys. Rev. Lett.* 65 895
[5] Thromat N, Noguera C, Gautier M, Jollet F and Duraud J P 1991 *Phys. Rev.* B **44** 7904
[6] Brydson R, Garvie L A, Craven A J, Sauer H, Hofer F and Cressey G 1993 *J. Phys.: Condens. Matter* **5** 9379
de Groot F M F, Figueiredo M O, Basto M J, Abbate M, Petersen H and Fuggle J C 1992 *Phys. Chem. Minerals* **19** 140
[7] Zaanen J, Sawatzky G A and Allen J W 1985 *Phys. Rev. Lett.* **55** 418
[8] de Groot F M F 1993 *J. Electron. Spectrosc. Relat. Phenom.* **62** 111
[9] Griffith J S 1961 *The Theory of Transition Metal Ions* (Cambridge: Cambridge University Press)
[10] de Groot F M F, Fuggle J C, Thole B T and Sawatzky 1990 *Phys. Rev.* B **42** 5459
van der Laan G and Kirkman I W 1992 *J. Phys.: Condens. Matter* **4** 4189
[11] Parlebas J C 1992 *J. Physique I* **2** 1369
Bocquet A E, Saitoh T, Mizokawa T and Fujimori A 1992 *Solid State Commun.* **83** 11
Fujomori A, Saeki M, Kimizuka N, Taniguchi M and Suga S 1986 *Phys. Rev.* B **34** 7318
van Veenendaal M A and Sawatzky G A 1993 *Phys. Rev. Lett.* **70** 2459
Beaurepaire E, Kappler J P, Lewonczuk S, Ringeissen J, Khan M A, Parlebas J C, Iwamoto Y and Kotani A 1993 *J. Phys.: Condens. Matter* **5** 5841
[12] Beaurepaire E, Lewonczuk S, Ringeissen J, Khan M A, Parlebas J C, Uozumi T, Okada K and Kotani A 1993 *Europhys. Lett.* **22** 463
[13] van Elp J 1991 *PhD Thesis* University of Groningen
[14] Figgis B N 1966 *Introduction to Ligand Fields* (New York: Interscience) p 38
[15] Slater J C and Koster G F 1954 *Phys. Rev.* **94** 1498
[16] Harrison W A 1980 *Electronic Structure and the Properties of Solids* (San Francisco, CA: Freeman)
[17] Teo B K and Lee P A 1979 *J. Am. Chem. Soc.* **101** 2815
[18] Fuggle J C and Inglesfield J E 1992 *Unoccupied Electronic States (Topics in Applied Physics)* vol 69 (Berlin: Springer) appendix B, p 347
[19] de Groot F M F, Fuggle J C, Thole B T and Sawatzky G 1990 *Phys. Rev.* B **41** 928
[20] Wyckoff R 1951 *Crystal Structures* (New York: Interscience)